Influence of Bone Adaptation on Tendon-to-Bone Healing in Bone Tunnel after Anterior Cruciate Ligament Reconstruction in a Rabbit Model

Chun-Yi Wen,[1,2] Ling Qin,[1,2] Kwong-Man Lee,[3] Margaret Wan-Nar Wong,[1] Kai-Ming Chan[1,2]

[1]Department of Orthopaedics and Traumatology, Faculty of Medicine, The Chinese University of Hong Kong, Hong Kong SAR, China, [2]The Hong Kong Jockey Club Sports Medicine and Health Sciences Centre, Faculty of Medicine, The Chinese University of Hong Kong, Hong Kong SAR, China, [3]Lee-Hysan Clinical Research Laboratory, The Chinese University of Hong Kong, Hong Kong SAR, China

Received 7 October 2008; accepted 18 March 2009
Published online 6 May 2009 in Wiley InterScience (www.interscience.wiley.com). DOI 10.1002/jor.20907

ABSTRACT: Anterior cruciate ligament (ACL) reconstruction with placement of grafted tendon in bone tunnel is a common surgical procedure. Bone tunnel creation may result in stress shielding of postero-lateral regions of tibial tunnel. The present study was designed to characterize the changes of peri-graft bone and compare with tendon-to-bone (T-B) healing in spatial and temporal manners after ACL reconstruction in rabbit. Surgical reconstruction using digital extensor tendon in bone tunnel was performed on 48 rabbits. Twelve rabbits were sacrificed at 0, 2, 6, and 12 weeks postoperatively for radiological and histological examinations. Bone mass and microarchitecture at the anterior, posterior, medial, and lateral regions of tunnel wall at distal femur and proximal tibia were evaluated. Using peripheral quantitative computed tomography, a 26, 22, and 42% decrease in bone mineral density (BMD) relative to baseline was present in the medial region of the femoral tunnel and the posterior and lateral regions of the tibial tunnel, respectively, at week 12 postoperatively ($p < 0.05$). It was accompanied by a decrease in trabecular number and increase in trabecular spacing, the shift of platelike to rodlike trabeculae, and loss of anisotropy under micro-computed tomography evaluation. This finding was echoed by histology showing increased osteoclastic activities and poor T-B healing in these regions. In conclusion, the postoperative bone loss and associated poor T-B healing was region-dependent, which may result from adaptive changes after tunnel creation. © 2009 Orthopaedic Research Society. Published by Wiley Periodicals, Inc. J Orthop Res 27:1447–1456, 2009

Keywords: anterior cruciate ligament (ACL) reconstruction; bone mass; microarchitecture; peripheral quantitative computed tomography (pQCT); micro-computed tomography (micro-CT)

Anterior cruciate ligament (ACL) reconstruction with placement of grafted tendon in bone tunnel is a common surgical procedure.[1,2] The quality of tendon-to-bone (T-B) healing is predictive of the long-term outcome of ACL surgery.[3,4] Peri-graft bone provides the surfaces for grafted tendon anchorage. Recently, it was found that the T-B repair strength deteriorated with a decrease in bone mineral density (BMD) in phalangeal tunnel of canine.[5,6] It was also reported that the chondral callus formation during T-B healing was much more extensive in the trabecular-filled femoral tunnel than in the marrow-dominated tibial tunnel after medial collateral ligament (MCL) reconstruction in rabbit.[7] These findings suggested that T-B healing was associated with the changes in bone mass and microarchitecture.

Naturally, there are no sites in human beings or animals where a tendon or ligament goes into a bone tunnel; therefore, tunnel creation would disrupt initial stress distribution of bone under the influence of mechanical loading. Recently, Au et al.[8] predicted in a finite element analysis that bone tunnel creation would result in stress shielding at the posterior and lateral regions of tibial tunnel. According to Wolff's Law,[9] the persistent stress shielding in these regions might result in bone resorption, and interfere with T-B healing subsequently.[10] It was hypothesized that the post-operative bone adaptive changes and associated T-B healing were region-dependent.

The present study was designed to investigate the spatiotemporal changes of peri-graft bone mass and microarchitecture, and to compare radiological findings with histological findings of T-B healing following ACL reconstruction in rabbit. High-resolution multilayer peripheral quantitative computed tomography (pQCT) and micro-computed tomography (micro–CT) were employed.[11,12] Accordingly, the findings of this study will provide an insight into regional bone adaptive changes following ACL reconstruction for enhancement of T-B healing in sports medicine.

METHODS

Study Design

This experiment was approved by the Research Ethics Committee of authors' institute. A total of 48 skeletally mature female New Zealand white rabbits (26 week old; weight: 3.5–4.0 kg) were used in this study. ACL reconstructions with long digital extensor tendon graft were performed bilaterally with one reconstructed knee evaluated and reported in the present study. The rabbits were euthanized at 0 (baseline), 2, 6, and 12 weeks postoperatively, with 12 rabbits comprising each time point. At each time point, six femur-graft-tibia complexes were harvested for pQCT and routine histological evaluation; the other six were used for micro-CT and sequential fluorescence labeling evaluation.

Animal Surgery

The ACL reconstruction rabbit model was established according to an established surgical protocol.[13] In brief, the rabbis were operated on under general anesthesia with 10% ketamine/2% xylazine (Kethalar, 1 mL:1 mL) and sedation was maintained with 2.5% sodium phenobarbital injected intravenously (Sigma Chemical Co., St. Louis, MO).

Correspondence to: Kai Ming Chan, Chair Professor of Department of Orthopaedics and Traumatology, RM. 74025, S/F, Clinical Sciences Building, Prince of Wales Hospital, Shatin, The Chinese University of Hong Kong, N.T., Hong Kong SAR, China. T: (952) 2632 2083; F: (852) 2646 3020; E-mail: kaimingchan@cuhk.edu.hk

The long digital extensor tendon graft was harvested and graft preparation was done by removing the attached muscle and passing the holding sutures through each end of the tendon graft in an interdigitating whipstitch fashion. A medial parapatella arthrotomy was performed to expose the knee joint. The patella was then dislocated and the infrapatella fat pad was removed to expose the joint cavity. After the ACL was excised, femoral and tibial tunnels were created through the footprint of the original ACL. The graft was then inserted and routed through the bone tunnels via the holding sutures. After femoral fixation, the graft was preconditioned within knee with manually applied cyclic loads. The graft was fixed with maximum tension at 90° knee flexion at the extra-articular exits of the tunnel to the neighboring soft tissue by secure knots. The wound was closed in layers and wrapped with a dressing. The rabbits were allowed free cage activities after surgery. The femur-graft-tibia complexes were harvested for the subsequent examinations at the specific time points.

pQCT Evaluation

The volumetric BMD (mg/m^3) in the vicinity of the grafted tendon on both distal femur and proximal tibia was measured using a high resolution multi-layer pQCT (Densiscan 2000; Scanco Medical, Brüttisellen, Switzerland). In brief, the samples assumed a supine position, with the leg fully extended in an anterior-posterior position. The samples were secured in a suitable radiolucent cast to fix knee joint in the position of full extension for scanning. An anterior-posterior scout image was obtained under peel mode and the joint line was set as the reference; the continuous slices were taken from tunnel aperture to tunnel exit perpendicular to the long axis of the limb with slice thickness of 1 mm and voxel size of 0.3 mm/pixel. The middle slice was selected on distal femur and proximal tibia, respectively, for analysis. On the selected slice, four regions of 3×3 mm^2 squares on anterior, posterior, medial, and lateral sides of bone tunnel wall were defined for apparent BMD measurement. A standard IBT phantom (IBT: Institut fur Biomedizinische Technik of ETH/UNI Zurich) measurement was performed daily with three measurement values within the given reference ranges provided by the manufacturer. The inter-scans repeated measurements of apparent BMD had been conducted in a pilot study that showed a precision error of 1.2%.

Micro-CT Evaluation

Bone mass and microarchitecture were evaluated using a high resolution micro-CT (micro-CT-40; Scanco Medical). In brief, the samples were placed with their long axes in the vertical position and immobilized with a foam pad in a cylindrical sample holder. The continuous scans were prescribed perpendicular to the long axis of the limb at an isotropic resolution of 30 μm^3. The region of interest (ROI) of 3×3 mm^2 was defined at anterior, posterior, medial, and lateral regions of bone tunnel wall on the 2D slices, and a total of 100 continuous slices of 3 mm in thickness in each region were reconstructed respectively for subsequent analysis. The acquired 3D data set was first convoluted with a 3D Gaussian filter with a "width" and "support" equal to 1.2 and 2, respectively. Bone was segmented from the marrow and soft tissue for subsequent analyses using a global thresholding procedure. A threshold equal to or above 210 represented bone tissue; a threshold below 210 represented bone marrow and soft tissue. The parameters of bone mass and microarchitecture were evaluated using the built-in software of the micro-CT, including material BMD, the fraction of bone volume over tissue volume (BV/TV), trabecular number (Tb.N), trabecular thickness (Tb.Th), trabecular spacing (Tb.Sp), and degree of anisotropy (D.A). The accuracy of micro-CT for measurement of bone mass and microarchitecture correlates well with other measurement modalities ($R^2 = 0.59–0.96$), which has been well documented in previous studies.[14,15] In the present study, our pilot study confirmed a low precision error of 0.3% by the inter-scan repeated measurements of bone volume fraction.

Degree of anisotropy represented the degree to which trabeculae were oriented toward a specific direction. It was measured by determining the mean intercept length (MIL) of the principal axes of the ellipsoid as a function of direction.[16] The principal axes of the ellipsoid were directly related to the anisotropy of bone.[17] The primary degree of anisotropy (DA_{13}) was reported, which was the ratio of the primary and tertiary axes. The secondary degree of anisotropy (DA_{23}) was also reported, which was the ratio of the secondary and tertiary axes. A value of 1.0 for DA_{13} indicated overall bone material isotropy, or does not contain a preferred direction, and higher values of degree of anisotropy indicated that a structure contained a preferential material direction. A value of 1.0 for DA_{23} indicated transverse bone material isotropy. The eigenvalues of the fabric tensor were normalized by the trace of fabric tensor and reported for comparison.

Histological Examination

The specimens were decalcified and embedded in wax. Cross sections 7 μm thick were cut perpendicular to the long axis of the bone tunnel and stained with hematoxylin-eosin. Under microscopic examination, T-B healing quality at the anterior, posterior, medial, and lateral region of the tunnel was graded morphologically on fibrocartilage formation, new bone formation, and T-B collagen fiber reconnection using a simplified Yeh et al.[18] method, in which 0, 1, and 2 represented the healing status of none, presence, and massive formation, respectively.

Sequential Fluorescence Labeling

Peri-graft bone mineral apposition was examined via sequential fluorescent dye labeling in vivo using our established protocol.[19] In brief, two fluorescent dyes, xylenol orange (90 mg/kg body weight) and calcein green (10 mg/kg body weight, both from Sigma-Aldrich GmbH), were injected subcutaneously and sequentially into the rabbits of the 6 week group at week 3 and 4, and of the 12 week group at week 9 and 10 postoperatively. After euthanasia, the specimens were fixed by wires after the adjustment of long axes of bone tunnel perpendicular to the ground, and then suspended in methylmethacrylate solution in plastic container for embedding. The specimens were sectioned perpendicularly to the bone tunnels. The sections in the middle portion of bone tunnel were grounded and polished to 80–100 μm by grinder/polisher (RotoPol-21; Struers, Denmark) for fluorescence microscopic examination. The labeled bone surfaces by red and green at the anterior, posterior, medial, and lateral regions of the tunnel were measured using MetaMorph Image Analysis System 6.3 (Universal Imaging Corp., Molecular Devices, Downingtown, PA). The fraction of labeled bone surface/total bone surface was calculated for comparison.

Statistical Analysis

The comparisons for bone mass, microarchitecture, and the fraction of the labeled bone surfaces among the

different time points and different regions (anterior, posterior, medial, lateral) were performed using two-way ANOVA in distal femur and proximal tibia. The comparison for the score of T-B healing quality was done using the Friedman test (nonparametric two-way ANOVA). When overall significance of main effects was indicated without interaction, multiple comparisons were performed among different time points in each region after Bonferroni correction. The level of significance was set at $p < 0.05$. All data analyses were performed using SPSS 15.0 analysis software (SPSS Inc., Chicago, IL).

RESULTS

pQCT Evaluation

The postoperative changes of apparent BMD varied at different regions of bone tunnel wall in both distal femur and proximal tibia ($p < 0.05$ for both) (Fig. 1).

At the anterior region around femoral tunnel, there were no significant differences in BMD among specific time points. At the posterior and anterior regions, BMD was significantly higher at week 2 and dropped back to the baseline level at week 6 after surgery; BMD at the lateral region was higher than the baseline at week 12 after surgery ($p < 0.05$ for all). A decrease in BMD was present in the medial region of femoral tunnel, where BMD significantly dropped at weeks 2 and 6 without further decrease at week 12; BMD was lower at week 12 postoperatively than the baseline by 26% ($p < 0.05$ for all).

At anterior and medial regions around the tibial tunnel, there was no significant change in the BMD among specific time points. A decrease in BMD occurred at the posterior and lateral regions. At the posterior region, BMD significantly dropped at weeks 2 and 6 without further decrease at week 12 postoperatively; it was lower at week 12 than the baseline by 22%

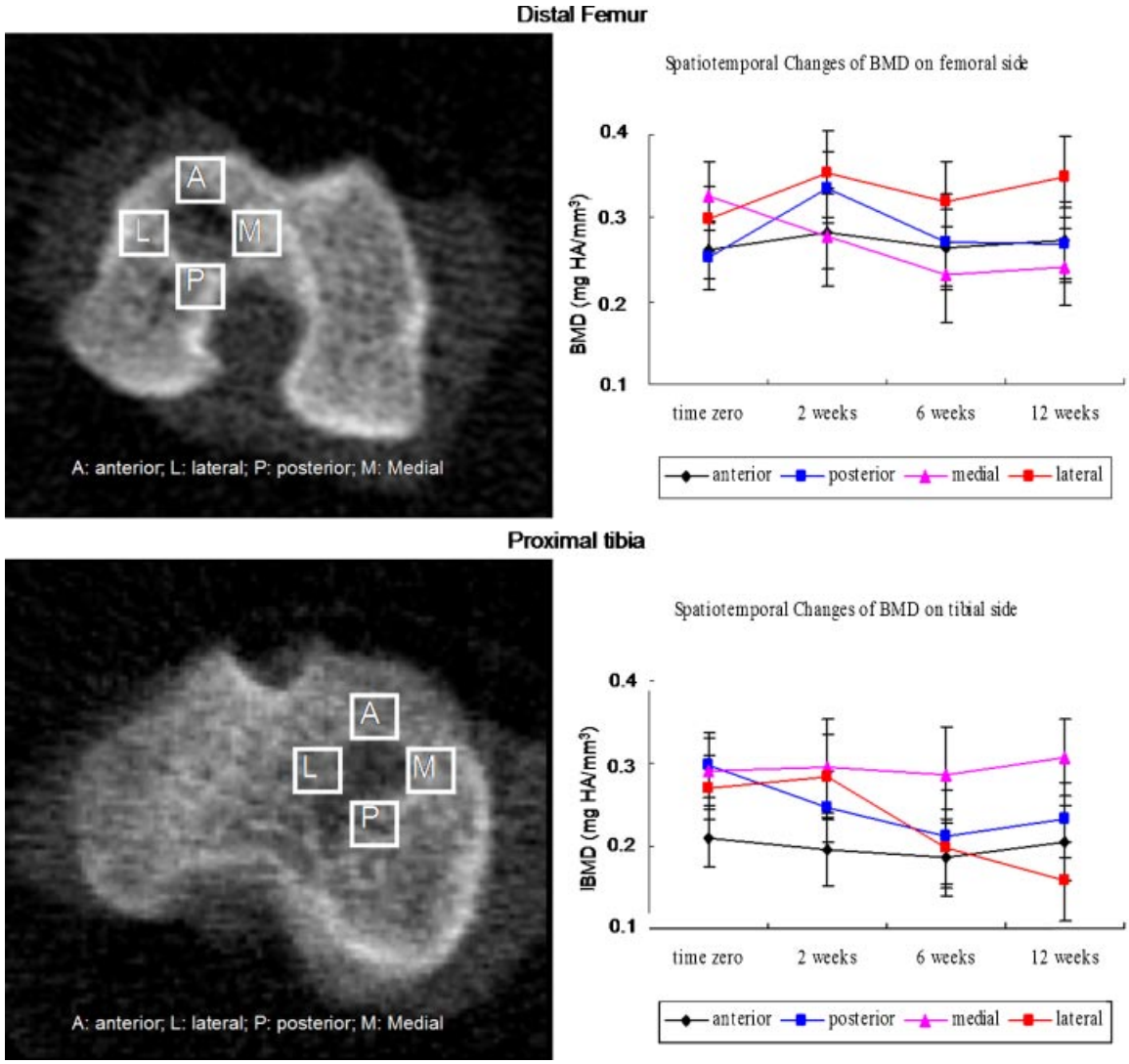

Figure 1. pQCT scan and examination. The cross section of distal femur and proximal tibia were taken and four regions of $3 \times$ mm^2 square on anterior, posterior, medial and lateral sides of bone tunnel was defined for evaluation of bone mineral density (BMD). The results showed that the changes of BMD were not uniform with healing over time around femoral and tibial tunnel. In distal femur, BMD significantly dropped at the medial region from week 2 till 6 and remained lower at week 12 after surgery than the baseline. BMD was higher at the posterior and lateral regions at week 2 and dropped back to the baseline level at week 6 after surgery, and it slightly increased at the lateral region at week 12 postoperatively. In proximal tibia, BMD decreased at the posterior region from week 2 till 6 and remained lower at week 12 after surgery than the baseline; BMD significantly dropped at the lateral region from week 6 to 12 postoperatively.

($p < 0.05$ for all). At the lateral region, BMD significantly decreased at weeks 6 and 12 after surgery; it was lower at week 12 postoperatively than the baseline by 42% ($p < 0.05$ for all).

Micro-CT Evaluation

The postoperative changes of material BMD and bone microarchitecture varied at different regions of bone tunnel on both distal femur and proximal tibia ($p < 0.05$ for both) (Fig. 2 and Table 1).

In distal femur, the postoperative bone loss occurred at the medial region, showing a decrease in BV/TV and Tb.N and an increase in Tb.Sp. BV/TV was lower than the baseline by 33% without a decrease in material BMD ($p < 0.05$) at week 12 postoperatively. At the lateral region, BV/TV increased with healing over time, with an increase in Tb.N and a decease in Tb.Sp. At the anterior and posterior regions, BV/TV was higher at week 2 postoperatively than the baseline, which was accompanied by an increase in Tb.N and a decrease in Tb.Sp; there were no significant differences afterwards in comparison with the baseline.

In proximal tibia, the postoperative bone loss was present at posterior and lateral regions, with a decrease in BV/TV and Tb.N and an increase in Tb.Sp. BV/TV was lower than the baseline at posterior and lateral regions by 32 and 28% at week 12 postoperatively ($p < 0.05$ for both). The decrease in material BMD occurred at lateral regions ($p < 0.05$). At the anterior and medial regions around the tibial tunnel, there were no significant

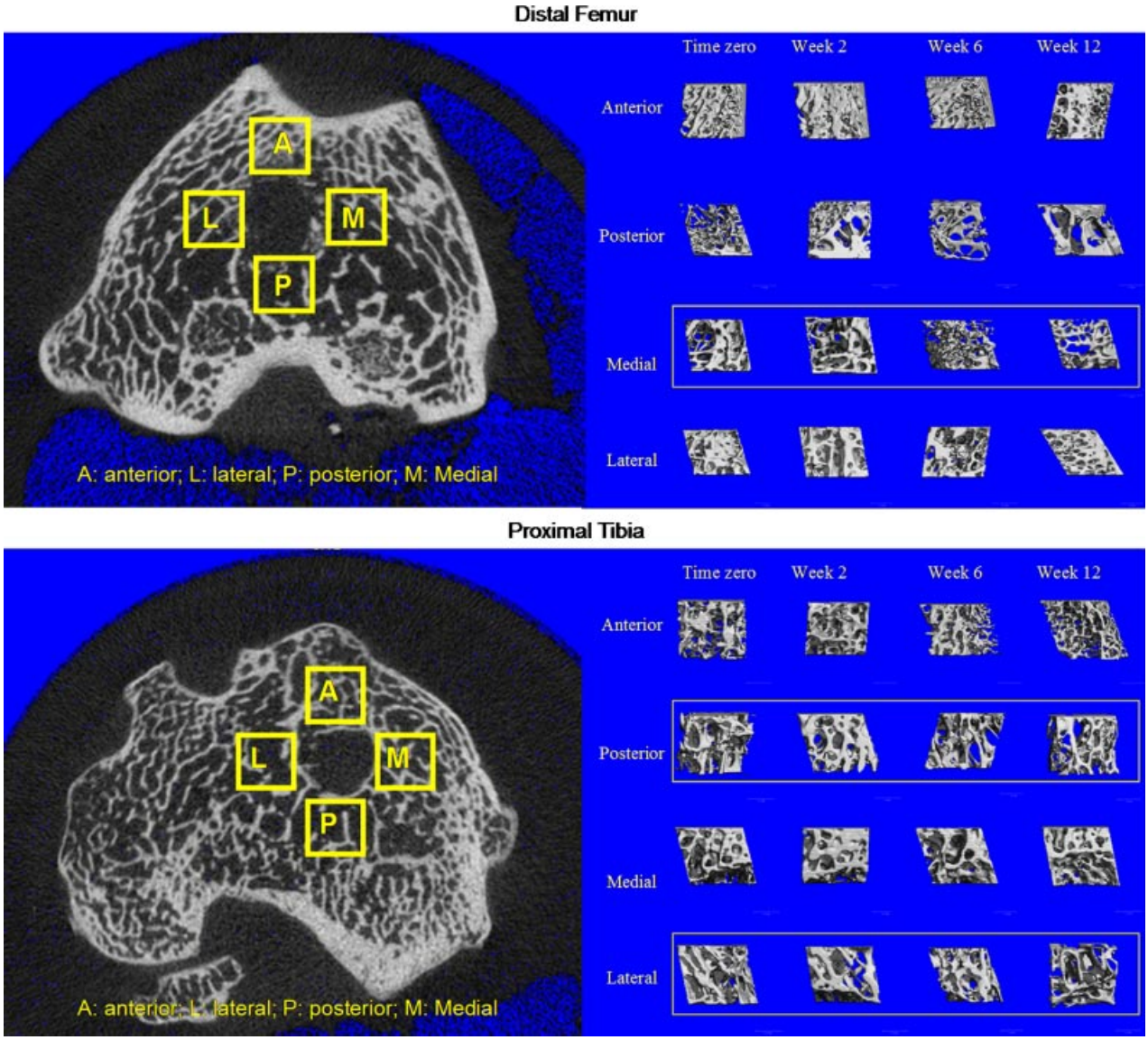

Figure 2. Micro-CT scan and examination. The cross section of distal femur and proximal tibia were taken and four regions of 3×3 mm^3 cube on anterior, posterior, medial and lateral sides of bone tunnel was defined for evaluation of bone mass and microarchitecture. The results showed that the postoperative bone loss was not uniform with healing over time around both the femoral and tibil tunnel. Significant bone loss was noted at the medial region around the femoral tunnel and the posterior and lateral regions of the tibial tunnel with healing over time (Box).

Table 1. Summary of Spatiotemporal Changes of Bone Mass and Microarchitecture Measured by Micro-CT, on Distal Femur and Proximal Tibia after ACL Reconstruction

			Material BMD (mg HA/mm^3)		BV/TV [%]		Tb.Th [mm]		Tb.Sp [mm]		Tb.N [/1mm]	
Site	Region	Group	Mean (S.D.)	δ	Mean (S.D.)	δ	Mean (S.D.)	δ	Mean (S.D.)	δ	Mean (S.D.)	δ
Femur	Anterior	Week 0	0.72 (0.03)	N/A	45.93 (3.84)	N/A	0.25 (0.02)	N/A	0.35 (0.03)	N/A	2.54 (0.14)	N/A
		Week 2	0.72 (0.05)	↔	54.05 (6.73)	↑	0.24 (0.02)	↔	0.27 (0.05)	↓	2.87 (0.22)	↑
		Week 6	0.73 (0.04)	↔	44.37 (4.39)	↔	0.22 (0.04)	↔	0.35 (0.04)	↔	2.60 (0.35)	↔
		Week 12	0.72 (0.04)	↔	49.53 (4.83)	↔	0.23 (0.03)	↔	0.32 (0.05)	↔	2.51 (0.29)	↔
	Posterior	Week 0	0.72 (0.02)	N/A	9.62 (1.93)	N/A	0.17 (0.02)	N/A	0.86 (0.06)	N/A	1.39 (0.10)	N/A
		Week 2	0.72 (0.04)	↔	12.40 (3.42)	↑	0.17 (0.03)	↔	0.71 (0.08)	↓	1.44 (0.19)	↔
		Week 6	0.70 (0.03)	↔	10.75 (2.37)	↔	0.18 (0.04)	↔	0.77 (0.10)	↔	1.39 (0.35)	↔
		Week 12	0.72 (0.05)	↔	10.03 (4.43)	↔	0.18 (0.04)	↔	0.78 (0.09)	↔	1.22 (0.31)	↔
	Medial #	Week 0	0.73 (0.02)	N/A	25.79 (2.16)	N/A	0.18 (0.02)	N/A	0.61 (0.05)	N/A	1.50 (0.16)	N/A
		Week 2	0.72 (0.04)	↔	20.07 (3.48)	↓	0.20 (0.03)	↔	0.64 (0.08)	↔	1.47 (0.23)	↔
		Week 6	0.69 (0.03)	↓	14.88 (3.54)	↓	0.12 (0.03)	↔	0.62 (0.08)	↔	1.30 (0.36)	↔
		Week 12	0.70 (0.04)	↔	17.11 (5.66)	↓	0.14 (0.05)	↔	1.04 (0.10)	↑	1.00 (0.30)	↓
	Lateral *	Week 0	0.73 (0.02)	N/A	20.92 (3.97)	N/A	0.16 (0.02)	N/A	0.54 (0.04)	N/A	1.70 (0.20)	N/A
		Week 2	0.72 (0.05)	↔	26.95 (5.25)	↑	0.17 (0.03)	↔	0.47 (0.05)	↓	1.82 (0.35)	↔
		Week 6	0.74 (0.05)	↔	25.72 (4.12)	↑	0.17 (0.03)	↔	0.49 (0.05)	↓	1.92 (0.33)	↔
		Week 12	0.72 (0.04)	↔	29.95 (4.26)	↑	0.18 (0.03)	↔	0.40 (0.08)	↓	2.13 (0.38)	↑
Tibia	Anterior	Week 0	0.68 (0.03)	N/A	19.64 (4.38)	N/A	0.16 (0.02)	N/A	0.48 (0.04)	N/A	2.45 (0.19)	N/A
		Week 2	0.70 (0.04)	↔	16.73 (7.85)	↔	0.15 (0.03)	↔	0.44 (0.05)	↔	2.31 (0.32)	↔
		Week 6	0.71 (0.05)	↔	14.60 (6.53)	↔	0.14 (0.03)	↔	0.47 (0.07)	↔	2.01 (0.43)	↔
		Week 12	0.73 (0.05)	↔	16.45 (7.12)	↔	0.12 (0.03)	↔	0.41 (0.05)	↔	2.28 (0.37)	↔
	Posterior #	Week 0	0.73 (0.03)	N/A	30.56 (5.35)	N/A	0.23 (0.05)	N/A	0.55 (0.05)	N/A	1.68 (0.31)	N/A
		Week 2	0.72 (0.05)	↔	25.10 (3.22)	↓	0.21 (0.03)	↔	0.63 (0.03)	↑	1.50 (0.22)	↔
		Week 6	0.71 (0.04)	↔	17.98 (4.98)	↓	0.20 (0.05)	↔	1.00 (0.06)	↑	0.96 (0.25)	↓
		Week 12	0.70 (0.04)	↔	20.77 (4.23)	↓	0.22 (0.04)	↔	0.72 (0.05)	↑	1.18 (0.32)	↓
	Medial	Week 0	0.71 (0.03)	N/A	33.81 (5.25)	N/A	0.20 (0.03)	N/A	0.45 (0.03)	N/A	1.91 (0.28)	N/A
		Week 2	0.73 (0.04)	↔	41.23 (7.42)	↑	0.24 (0.04)	↑	0.41 (0.05)	↔	2.07 (0.45)	↔
		Week 6	0.75 (0.04)	↔	30.97 (5.18)	↔	0.19 (0.04)	↔	0.52 (0.05)	↔	1.80 (0.30)	↔
		Week 12	0.74 (0.05)	↔	34.09 (5.45)	↔	0.19 (0.03)	↔	0.45 (0.05)	↔	1.94 (0.21)	↔
	Lateral #	Week 0	0.75 (0.03)	N/A	26.28 (4.72)	N/A	0.17 (0.02)	N/A	0.53 (0.04)	N/A	1.69 (0.29)	N/A
		Week 2	0.74 (0.05)	↔	21.43 (6.26)	↔	0.20 (0.03)	↔	0.57 (0.07)	↔	1.27 (0.35)	↓
		Week 6	0.72 (0.03)	↓	18.76 (5.81)	↓	0.16 (0.02)	↔	0.69 (0.06)	↑	1.33 (0.37)	↓
		Week 12	0.69 (0.05)	↓	18.69 (5.27)	↓	0.18 (0.02)	↔	0.78 (0.06)	↑	1.32 (0.34)	↓

The means and S.D. for each site, region and group are shown). A positive or negative difference (δ) was represented by an upward arrow downward arrow, respectively if the difference was statistically significant ($p < 0.05$) in each region between the specific time points and the baseline via multiple comparisons after two-way factorial ANOVA. "#" ("*") indicated the specific regions around bone tunnel with the significant bone loss or gain.

differences at weeks 6 and 12 in comparison with the baseline although significant changes of bone were present at week 2 after surgery.

As shown in Table 2, a decrease of 12% in the overall fabric anisotropy was detected at the medial region around the femoral tunnel at week 12 after surgery ($p < 0.05$). At the proximal tibia, a decrease in the overall fabric anisotropy was also detected at posterior and lateral regions by 15 and 20%, respectively, at week 12 post-operatively ($p < 0.05$ for both). Meanwhile, the decrease in transverse fabric anisotropy was only found at the lateral region around the tibial tunnel after surgery.

Histological Examination

T-B healing varied at different regions of bone tunnel (Fig. 3). In femoral tunnel, there existed two types of T-B healing interface tissue: cartilaginous and fibrous. At the lateral region in the femoral tunnel, the cartilaginous healing interface tissue was present at week 2 and was gradually replaced by bone in-growth at week 6, then the T-B collagen fiber reconnection was re-established at week 12 postoperatively. The fibrous interface tissue occurred at the other regions of the femoral tunnel. Fibrous healing interface narrowed with healing over time and grafted tendon directly connected with bone tunnel with sparse collagen fibers at week 12 postoperatively. The perfect score of T-B healing quality at lateral region (median/[range]: 6[5,6]) was highest in femoral tunnel at week 12 after surgery ($p < 0.05$ for all).

Fibrous interface tissue was dominant in the tibial tunnel. At the posterior and lateral regions, fibrovascular tissue was present at week 2 post-operatively; osteoclasts accumulated at the bone surface at week 6 after surgery; and the grafted tendon connected with bone tunnel indirectly via fibrous healing interface tissue at week 12 after surgery, where the score of T-B healing quality was lower than in the other two regions (posterior: 2[1,3] and lateral: 2[1,2] vs. anterior: 3[2,4] and medial: 4[3,4]) ($p < 0.05$ for all).

Sequential Fluorescence Labeling Examination

The disparity of the activities of mineral apposition around the bone tunnel was similarly observed at weeks 6 and 12 after surgery. As shown in Figure 4, the fraction of the labeled bone surfaces at the medial region was lowest ($15 \pm 4\%$) around the femoral tunnel (anterior: $22 \pm 5\%$; posterior: $20 \pm 4\%$; and lateral: $29 \pm 7\%$). Around the tibial tunnel, the fractions of the labeled bone surfaces on posterior ($11 \pm 5\%$) and lateral regions ($8 \pm 3\%$) were significantly lower than anterior ($19 \pm 6\%$) and medial regions ($18 \pm 5\%$) at week 6 postoperatively ($p < 0.05$ for all).

DISCUSSION

Clinically, a decrease in BMD has been reported after ACL reconstruction using 2D dual-energy X-ray absorptiometry (DEXA).[20–22] The present study was the first to employ the 3D advanced imaging tools pQCT and micro-CT for evaluation of volumetric BMD and bone microarchitecture of the corresponding bony regions around the tunnel. Our findings suggested that the decrease in BMD revealed by DEXA might occur at specific regions, that is, the posterior and lateral regions of the tibial tunnel wall, instead of a uniform decrease. In addition, the apparent bone mineral loss resulted from the decrease in trabecular number and the increase in trabecular spacing and the material BMD loss. Actually, the regional variation of bone loss has been noted clinically but it was not highlighted in Zerahn et al.'s study.[20] They reported that the significant decrease in BMD occurred in the lateral region of the tibia after ACL reconstruction with BMD at the medial region within normal range.

Such region-dependent bone loss might be associated with the altered mechanical milieus after tunnel creation. Micro-CT data could provide unique information on fabric anisotropy of bone, which reflects its structure preferentially along certain directions of mechanical loading.[23] Our results showed that the overall fabric anisotropy of bone decreased at the medial region around the femoral tunnel and the posterior and lateral regions of the tibial tunnel. The results indicated the reduction or loss of specific direction mechanical loading in these regions. These findings were consistent with Au et al.'s study.[8] They predicted stress shielding at the posterior and lateral regions of the tibial tunnel with the loading along the long axis of the proximal tibia in a finite element model. The persistent stress shielding would result in bone resorption according to Wolff's Law.[9] In addition, the fabric anisotropy of bone was more severely affected at the lateral region of the tibial tunnel, as the transverse anisotropy of bone decreased as well as the overall anisotropy. This might explain why bone loss was more severe at the lateral region of the tibial tunnel at week 12 after surgery.

The region-dependent bone loss under pQCT and micro-CT evaluation was echoed by the histological findings. It was observed that osteoclasts accumulated at the surface of bone at the specific region, that is, the lateral region of the tibial tunnel, with healing over time. Increased osteoclastic activities were accompanied by less bone mineral apposition and poor T-B healing. Rodeo et al.[10] evaluated the role of osteoclastic bone resorption in T-B healing after ACL reconstruction in rabbit by modulating osteoclastic activities using osteoprotegerin and the receptor activator of nuclear factor-kappa B ligand. Activation of osteoclasts resulted in less peri-graft bone and a decrease of the stiffness of T-B complexes.[10]

Bisphosphonate, an inhibitor of bone resoprtion, has been studied in an attempt to augment T-B healing in bone tunnel.[5,24] Although satisfactory results were shown after systemic administration of bisphosphonates, our histomorphological evaluation implied that local administration, that is, at the posterior and lateral regions of the tibial tunnel, would be more

Table 2. Summary of Fabric Anisotropic Changes of Bone Measured by Micro-CT on Distal Femur and Proximal Tibia after ACL Reconstruction

			H1	H2	H3	DA_{13}		DA_{23}	
Site	Region	Group	Mean (S.D.)	Mean (S.D.)	Mean (S.D.)	Mean (S.D.)	δ	Mean (S.D.)	Δ
Femur	Anterior	Week 0	0.39 (0.01)	0.36 (0.01)	0.25 (0.01)	1.55 (0.10)	N/A	1.41 (0.05)	N/A
		Week 2	0.39 (0.01)	0.35 (0.01)	0.26 (0.01)	1.53 (0.13)	↔	1.35 (0.09)	↔
		Week 6	0.42 (0.02)	0.36 (0.02)	0.22 (0.01)	1.66 (0.21)	↔	1.40 (0.08)	↔
		Week 12	0.40 (0.02)	0.35 (0.01)	0.25 (0.01)	1.56 (0.17)	↔	1.38 (0.06)	↔
	Posterior	Week 0	0.40 (0.01)	0.33 (0.01)	0.27 (0.01)	1.46 (0.05)	N/A	1.22 (0.04)	N/A
		Week 2	0.37 (0.02)	0.35 (0.02)	0.28 (0.01)	1.47 (0.15)	↔	1.22 (0.08)	↔
		Week 6	0.39 (0.01)	0.35 (0.02)	0.26 (0.01)	1.51 (0.08)	↔	1.27 (0.12)	↔
		Week 12	0.42 (0.01)	0.31 (0.01)	0.27 (0.01)	1.54 (0.09)	↔	1.23 (0.06)	↔
	Medial #	Week 0	0.41 (0.01)	0.35 (0.01)	0.25 (0.01)	1.65 (0.06)	N/A	1.42 (0.09)	N/A
		Week 2	0.38 (0.02)	0.37 (0.02)	0.25 (0.02)	1.54 (0.09)	↔	1.48 (0.06)	↔
		Week 6	0.39 (0.01)	0.34 (0.02)	0.27 (0.02)	1.46 (0.08)	↓	1.45 (0.07)	↔
		Week 12	0.39 (0.01)	0.33 (0.22)	0.28 (0.01)	1.45 (0.12)	↓	1.46 (0.10)	↔
	Lateral	Week 0	0.42 (0.01)	0.38 (0.01)	0.20 (0.01)	2.02 (0.10)	N/A	1.94 (0.05)	N/A
		Week 2	0.44 (0.02)	0.37 (0.01)	0.20 (0.01)	2.08 (0.10)	↔	1.91 (0.08)	↔
		Week 6	0.42 (0.02)	0.37 (0.01)	0.20 (0.01)	2.05 (0.08)	↔	1.83 (0.08)	↔
		Week 12	0.42 (0.02)	0.36 (0.01)	0.22 (0.01)	1.94 (0.09)	↔	1.87 (0.09)	↔
Tibia	Anterior	Week 0	0.42 (0.01)	0.30 (0.01)	0.29 (0.01)	1.46 (0.07)	N/A	1.03 (0.08)	N/A
		Week 2	0.39 (0.02)	0.33 (0.01)	0.28 (0.01)	1.40 (0.10)	↔	1.09 (0.06)	↔
		Week 6	0.39 (0.01)	0.31 (0.01)	0.30 (0.01)	1.40 (0.11)	↔	1.02 (0.05)	↔
		Week 12	0.42 (0.01)	0.30 (0.02)	0.28 (0.01)	1.50 (0.09)	↔	1.08 (0.06)	↔
	Posterior #	Week 0	0.42 (0.01)	0.30 (0.01)	0.28 (0.01)	1.50 (0.06)	N/A	1.07 (0.04)	N/A
		Week 2	0.38 (0.02)	0.33 (0.02)	0.30 (0.01)	1.58 (0.08)	↔	1.10 (0.08)	↔
		Week 6	0.40 (0.02)	0.31 (0.02)	0.29 (0.02)	1.38 (0.14)	↓	1.09 (0.05)	↔
		Week 12	0.42 (0.02)	0.32 (0.02)	0.26 (0.01)	1.27 (0.15)	↓	1.21 (0.09)	↑
	Medial	Week 0	0.41 (0.01)	0.34 (0.01)	0.25 (0.01)	1.56 (0.07)	N/A	1.32 (0.06)	N/A
		Week 2	0.41 (0.02)	0.31 (0.01)	0.28 (0.01)	1.52 (0.08)	↔	1.31 (0.09)	↔
		Week 6	0.40 (0.01)	0.34 (0.02)	0.26 (0.01)	1.53 (0.12)	↔	1.33 (0.10)	↔
		Week 12	0.42 (0.01)	0.33 (0.01)	0.25 (0.01)	1.59 (0.14)	↔	1.34 (0.09)	↔
	Lateral #	Week 0	0.41 (0.01)	0.34 (0.01)	0.24 (0.01)	1.71 (0.09)	N/A	1.41 (0.08)	N/A
		Week 2	0.41 (0.02)	0.33 (0.01)	0.26 (0.02)	1.54 (0.12)	↓	1.26 (0.06)	↓
		Week 6	0.41 (0.02)	0.32 (0.02)	0.27 (0.02)	1.56 (0.15)	↓	1.21 (0.07)	↓
		Week 12	0.38 (0.01)	0.35 (0.02)	0.28 (0.01)	1.36 (0.23)	↓	1.25 (0.09)	↓

The eigenvalues of the fabric tensor (H1, H2, H3) are the means and S.D for each site, region and group. A positive or negative difference (δ) of tabric anisotropy was represented by an upward arrow or downward arrow, if the difference was statistically significant ($p < 0.05$) in each region between the specific time points and the baseline via multiple comparisons after two-way ANOVA. Eigenvalues had been normalized by the trace of the fabric tensor (H1+H2+H3). "#" indicated the specific regions around bone tunnel with the significant change in fabric anisotropy.

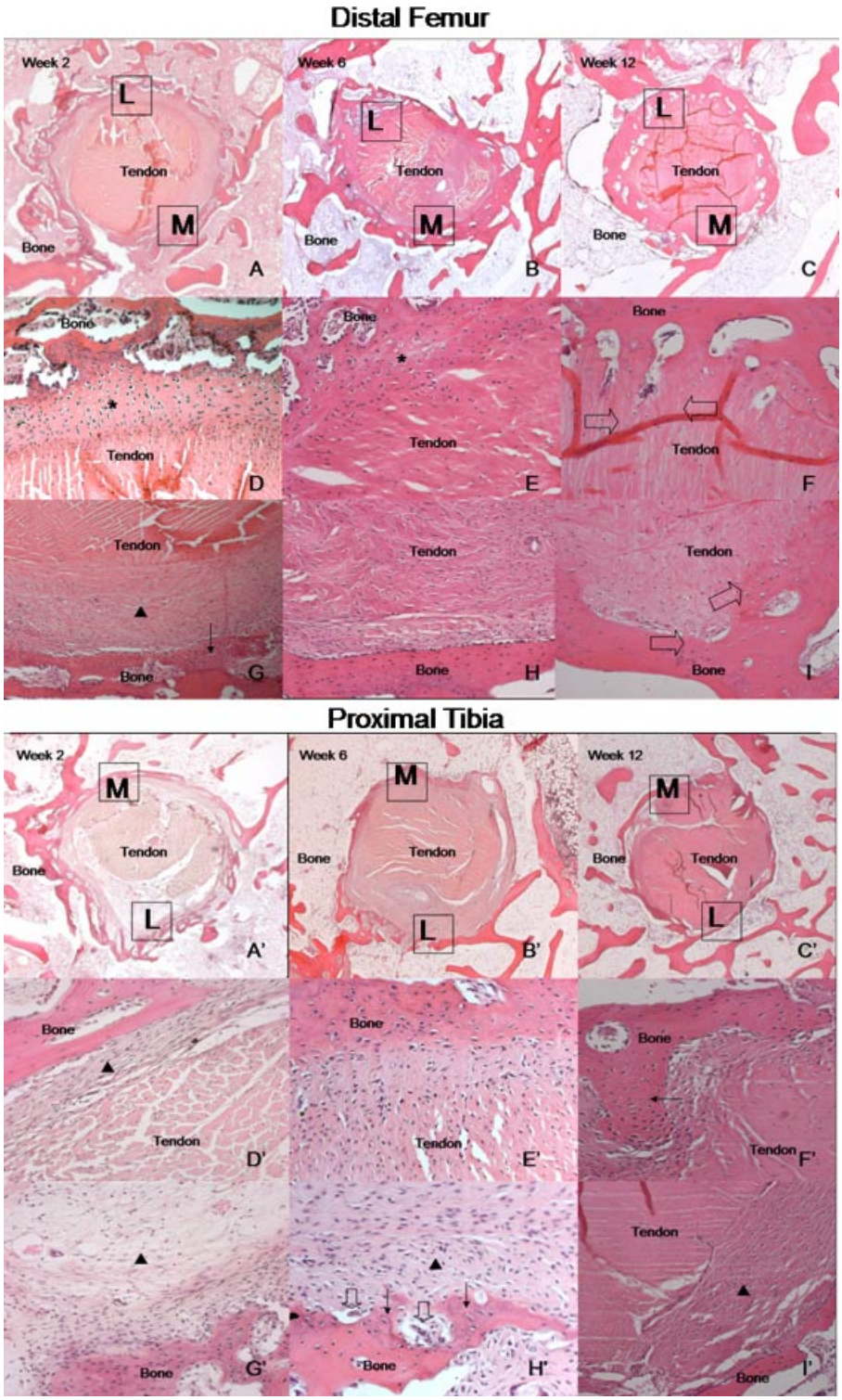

Figure 3. The representative images showing the spatiotemporal changes of tendon-to-bone healing in femoral and tibial tunnel at low (A–C and A'–C', 16X) and high magnification (D–I and D'–I', 200X). The medial region of femoral tunnel and the lateral region of tibial tunnel, where bone was more seriously affected, were shown here with the opposite regions for comparison (M: medial; L: lateral). At the lateral region of the femoral tunnel, cartilaginous healing tissue (*) was present at the T-B healing interface at week 2 after surgery (D); chondrocytes at the healing interface became aligned along the collagen fibers from bone to tendon at week 6 (E); it was gradually replaced by in-growth bone with reestablishment of direct T-B bond (block arrow, F). At the medial region of femoral tunnel, fibrous tissue (triangle) was present T-B healing interface at week 2 after surgery with new bone formation (arrow, G); fibrous healing interface narrowed at week 6 with healing over time (H). Direct collagen fibers connection from bone to tendon (block arrow) was observed at week 12 postoperatively (I). At medial region of tibial tunnel, loose fibrous tissue (triangle) was present at T-B healing interface at week 2 after surgery (D'); fibrous tissue became dense at week 6 (E'); it was gradually replaced by bone in-growth (arrow) with reestablishment of direct T-B collagen fibers connection (F'). At the lateral region of the tibial tunnel, fibrovascular tissue (triangle) was present T-B healing interface at week 2 after surgery (G'); osteoclasts (block arrow) accumulated at bone surface at week 6 postoperatively, which coupled with osteoblastic activity and osteoid formation (arrow, H'); there formed indirect T-B contact formation via fibrous interface tissue at week 12 after surgery (I').

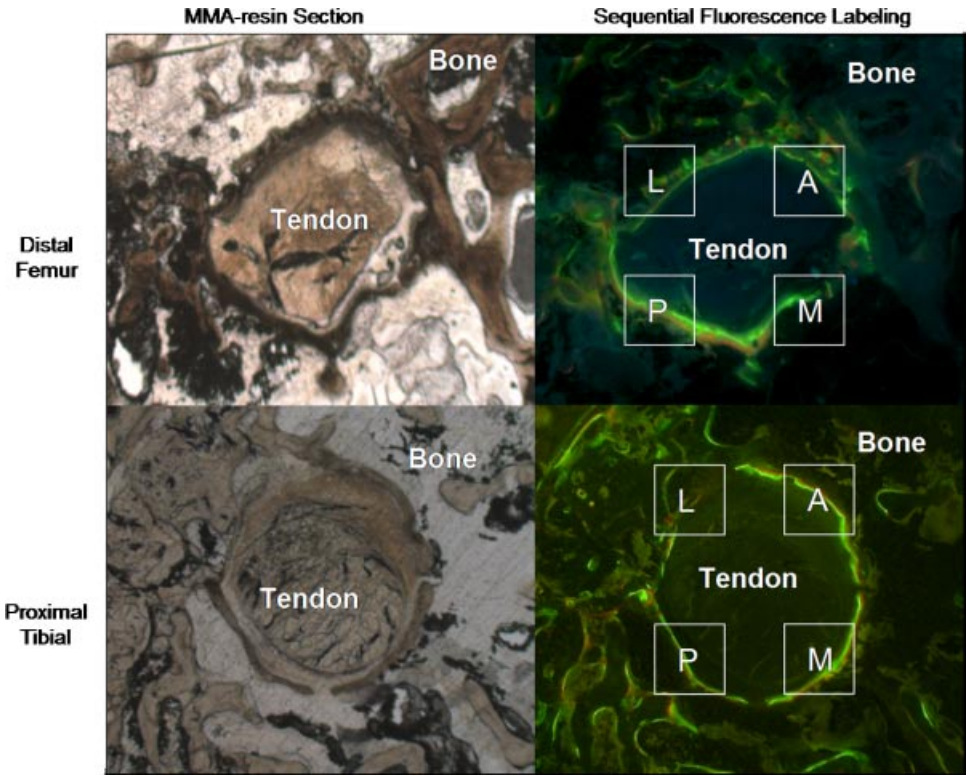

Figure 4. Representative images showing that bone mineral apposition was not uniform around the femoral and tibial tunnel at week 6 after surgery. In distal femur, the fraction of fluorescence-labeled bone surface at the medial region was relatively less than the other regions. In proximal tibia, the fraction of labeled bone surface at the posterior and lateral regions was relatively less than the other regions (Original Magnification: 16X).

promising as bone resorption was region dependent. Furthermore, significant bone loss and increased osteoclastic activities were present in the first six weeks after surgery in our rabbit model. During the first 6 weeks, bone resorption impaired T-B healing and restricted the early motion postoperatively.[25] Thus, the time window in the first 6 weeks should be focused on augmentation of T-B healing via inhibition of bone resorption to facilitate early motion and accelerated rehabilitation.

A disparity between bone adaptive changes and associated T-B healing was also found in the present study. It was shown that the cartilaginous interface tissue occurred in the femoral tunnel and the fibrous interface tissue was dominant in the tibial tunnel in our rabbit ACL reconstruction model. During T-B healing in the femoral tunnel, such cartilaginous interface tissue was gradually replaced by bone in-growth with establishment of direct T-B integration. This healing process resembled endochondral ossification, which is considered to be the developmental process of ACL-to-bone insertion.[26] Femoral tunnel with less pronounced bone loss might provide a relatively stable surface for graft anchorage in comparison with the tibial tunnel, which might explain such disparity of T-B healing in bone tunnels. This finding was consistent with Grassman et al.'s study.[7] They described two types of T-B healing interface tissue: cartilaginous and fibrous, which were present in trabeculae-rich (femoral) and trabeculae-poor (tibial) tunnels, respectively, after MCL reconstruction in rabbit. Bone resoprtion in the tibial tunnel, which was indicated by tunnel widening, was associated with knee laxity.[27] Thus, it should be targeted for enhancement.

In conclusion, the postoperative bone adaptive changes and associated T-B healing were region dependent, which might be associated with bone tunnel creation. Bone tunnel creation has a theoretical advantage in that it provides a large bone surface and facilitates T-B healing. However, our findings in the present study led us to rethink this traditional concept. Actually, tunnel creation disrupted the physiological mechanical loading, resulting in region-dependent stress shielding and subsequent bone loss, which then impaired T-B healing. Thus, bone resorption, particularly in the tibial tunnel, should raise our concerns on the security of grafted tendon anchorage in bone tunnel in clinical practice and be targeted for further enhancement in future studies.

ACKNOWLEDGMENTS

This study was supported by the Research Grant Council Earmarked Grants 06-07 (CUHK4497/06M), Hong Kong SAR, China. The authors would like to thank Po-Yee Lui and Sai-chuen Fu, who provided expertise at academic meetings, as well as Hui-Yan Yeung, Chun-Wai Chan, Grace Ho, and Anita Wai-Ting Shum, who provided technical assistance. The

authors would like to thank Qiu Hong for her assistance in statistical analysis.

REFERENCES

1. Fu FH, Bennett CH, Ma CB, et al. 2000. Current trends in anterior cruciate ligament reconstruction. Part II. Operative procedures and clinical correlations. Am J Sports Med 28: 124–130.
2. Fu FH, Bennett CH, Lattermann C, et al. 1999. Current trends in anterior cruciate ligament reconstruction. Part 1: Biology and biomechanics of reconstruction. Am J Sports Med 27:821–830.
3. Steiner ME, Murray MM, Rodeo SA. 2008. Strategies to improve anterior cruciate ligament healing and graft placement. Am J Sports Med 36:176–189.
4. Deehan DJ, Cawston TE. 2005. The biology of integration of the anterior cruciate ligament. J Bone Joint Surg Br 87:889–895.
5. Thomopoulos S, Matsuzaki H, Zaegel M, et al. 2007. Alendronate prevents bone loss and improves tendon-to-bone repair strength in a canine model. J Orthop Res 25:473–479.
6. Silva MJ, Thomopoulos S, Kusano N, et al. 2006. Early healing of flexor tendon insertion site injuries: Tunnel repair is mechanically and histologically inferior to surface repair in a canine model. J Orthop Res 24:990–1000.
7. Grassman SR, McDonald DB, Thornton GM, et al. 2002. Early healing processes of free tendon grafts within bone tunnels is bone-specific: a morphological study in a rabbit model. Knee 9:21–26.
8. Au AG, Raso VJ, Liggins AB, et al. 2005. A three-dimensional finite element stress analysis for tunnel placement and buttons in anterior cruciate ligament reconstructions. J Biomech 38:827–832.
9. Wolff J. 1986. The law of bone remodeling. Berlin: Springer.
10. Rodeo SA, Kawamura S, Ma CB, et al. 2007. The effect of osteoclastic activity on tendon-to-bone healing: an experimental study in rabbits. J Bone Joint Surg Am 89:2250–2259.
11. Siu WS, Qin L, Cheung WH, et al. 2004. A study of trabecular bones in ovariectomized goats with micro-computed tomography and peripheral quantitative computed tomography. Bone 35:21–26.
12. Hao YJ, Zhang G, Wang YS, et al. 2007. Changes of microstructure and mineralized tissue in the middle and late phase of osteoporotic fracture healing in rats. Bone 41:631–638.
13. Wang CJ, Wang FS, Yang KD, et al. 2005. The effect of shock wave treatment at the tendon-bone interface-an histomorphological and biomechanical study in rabbits. J Orthop Res 23:274–280.
14. MacNeil JA, Boyd SK. 2007. Accuracy of high-resolution peripheral quantitative computed tomography for measurement of bone quality. Med Eng Phys 29:1096–1105.
15. Ding M, Odgaard A, Hvid I. 1999. Accuracy of cancellous bone volume fraction measured by micro-CT scanning. J Biomech 32:323–326.
16. Whitehouse WJ. 1974. The quantitative morphology of anisotropic trabecular bone. J Microsc 101:153–168.
17. Odgaard A, Kabel J, van Rietbergen B, et al. 1997. Fabric and elastic principal directions of cancellous bone are closely related. J Biomech 30:487–495.
18. Yeh WL, Lin SS, Yuan LJ, et al. 2007. Effects of hyperbaric oxygen treatment on tendon graft and tendon-bone integration in bone tunnel: biochemical and histological analysis in rabbits. J Orthop Res 25:636–645.
19. Lu H, Qin L, Fok P, et al. 2006. Low-intensity pulsed ultrasound accelerates bone-tendon junction healing: a partial patellectomy model in rabbits. Am J Sports Med 34:1287–1296.
20. Zerahn B, Munk AO, Helweg J, et al. 2006. Bone mineral density in the proximal tibia and calcaneus before and after arthroscopic reconstruction of the anterior cruciate ligament. Arthroscopy 22:265–269.
21. Leppala J, Kannus P, Natri A, et al. 1999. Effect of anterior cruciate ligament injury of the knee on bone mineral density of the spine and affected lower extremity: a prospective one-year follow-Up study. Calcif Tissue Int 64:357–363.
22. Kannus P, Sievanen H, Jarvinen M, et al. 1992. A cruciate ligament injury produces considerable, permanent osteoporosis in the affected knee. J Bone Miner Res 7:1429–1434.
23. Odgaard A. 1997. Three-dimensional methods for quantification of cancellous bone architecture. Bone 20:315–328.
24. Hays PL, Kawamura S, Deng XH, et al. 2008. The role of macrophages in early healing of a tendon graft in a bone tunnel. J Bone Joint Surg Am 90:565–579.
25. Sakai H, Fukui N, Kawakami A, et al. 2000. Biological fixation of the graft within bone after anterior cruciate ligament reconstruction in rabbits: effects of the duration of postoperative immobilization. J Orthop Sci 5:43–51.
26. Nawata K, Minamizaki T, Yamashita Y, et al. 2002. Development of the attachment zones in the rat anterior cruciate ligament: changes in the distributions of proliferating cells and fibrillar collagens during postnatal growth. J Orthop Res 20:1339–1344.
27. Webster KE, Chiu JJ, Feller JA. 2005. Impact of measurement error in the analysis of bone tunnel enlargement after anterior cruciate ligament reconstruction. Am J Sports Med 33:1680–1687.